



Physical properties of nanoparticles do matter

Tony Mutiso Kiio¹ · Soyeun Park¹

Received: 3 April 2020 / Accepted: 7 October 2020 / Published online: 22 October 2020
© The Korean Society of Pharmaceutical Sciences and Technology 2020

Abstract

Background Nanoparticles (NPs) have been used to enhance pharmaceutical properties of drugs, including cell/tissue penetration, selective biodistribution, circulation half-life, and accumulation at target sites. Rigorous efforts, including chemical modifications using target moieties, have been dedicated to improving their functions.

Area covered Optimization of the physical properties of NPs, including size, shape, charge, and elasticity, is suggested to be an important step in the creation of NPs with desirable pharmacokinetic properties for use as drug delivery systems. In this review, we highlight recent findings on the effect of the physical properties of NPs, including the size, shape, surface charge, and elasticity on pharmaceutical functions.

Expert opinion Many studies have demonstrated that 30–200 nm NPs facilitate cell uptake and do not trigger the immune response due to their relatively large surface area. Compared to spherical NPs, non-spherical NPs are not only advantageous for cell uptake but also for systemic circulation owing to their multivalent interactions with the cell surface. The slightly negative charges carried by NPs have been considered responsible for the reduced electrostatic interactions with plasma proteins. Importantly, soft NPs enhance cellular uptake, reduce immunogenicity, and enhance tumor accumulation compared to their hard counterparts. Nonetheless, it is not easy to offer unequivocal suggestions regarding the physical properties of NPs during their pharmacokinetic journey; this is due to the multifaceted aspects at each step. Smart NPs that can alter their physical properties by responding to environmental stimuli were developed as alternatives to address this issue. Thus, physical properties do play a very important role in determining the pharmaceutical applications of NPs.

Keywords Elasticity · Nanoparticles · Pharmacokinetics · Size · Shape · Surface charge

Introduction

Nanomedicine incorporating nanoparticles (NPs) as drug delivery systems has had unprecedented growth in recent years. In fact, substantial efforts have been dedicated to the development of innovative drug carriers that can protect therapeutic agents from degradation, enhance efficacy, and alleviate side effects (Wang and Wang 2014). Numerous NP therapeutics have been approved by the FDA for clinical use, and several others are in late-phase clinical trials (Barenholz 2012; Davis et al. 2008; Jain and Stylianopoulos 2010). The NPs used in nanomedicine are in the range of 10–1000 nm. Several forms of NPs, such as liposomal NPs composed of phospholipids (Han et al. 2018; Lee 2019), polymeric NPs

synthesized using natural (e.g. gelatin, albumin) and synthetic polymers (e.g. polylactides, polyalkylcyanoacrylates) (Crucho and Barros 2017), inorganic NPs including silica NPs (Zheng et al. 2018), quantum dots (Probst et al. 2013), metal NPs (Vio et al. 2017), and lanthanide NPs (Shen et al. 2013b), have been established.

Emerging nanotechnology has revealed the unique physicochemical properties of NPs, which were unexpected due to their conventional bulk chemical equivalents. The unique features of NPs offer novel advantages such as membrane permeability, bioavailability, biodegradability, biocompatibility, metabolic stability, target delivery, and duration of action (Abdifetah and Na-Bangchang 2019). For instance, amphiphilic NPs such as liposomes and micelles exhibit enhanced permeability to the cell membrane (Liu et al. 2013; Zhao et al. 2015). In addition, the similarities between liposomal NPs and biological membranes allow high biodegradability and low immunogenicity. The high stability of NPs inherently results in a sustained release of the encapsulated

✉ Soyeun Park
syPark20@gmail.com

¹ College of Pharmacy, Keimyung University, 1095 Dalgubeoldaero, Daegu 42601, Republic of Korea

drug owing to their role as a shielding barrier. Some NPs improve the solubility of hydrophobic drugs, enhance drug efficacy, and reduce side effects (Kim et al. 2020; Patel et al. 2012; Singh et al. 2018). The prolonged circulation of NPs following parenteral administration increases their duration of action and improves their therapeutic efficacy. These advantages have markedly increased the use of NPs as vehicles for the delivery of various therapeutic agents, including antibiotics (Sousa et al. 2017), anti-rheumatic drugs (Van den Hoven et al. 2011), anti-inflammatory drugs (Koga et al. 2016), and anticancer drugs (Al-azzawi and Masheta 2019; Le et al. 2018; Sobh et al. 2019; Taghipour-Sabzevar et al. 2019).

Despite these advantages, some concerns emerge as the entry of NPs into the biological system triggers an immune response. The size of NPs used in nanomedicine is comparable to the size of the virus to which the innate immune system responds. Foreign substances, including NPs as well as viruses in systemic circulation, are eliminated by the mononuclear phagocyte system, also known as the reticuloendothelial system (RES). Immune cells such as monocytes in blood circulation and macrophages in different organs of the body, including the liver, spleen, lymph nodes, lungs, bone marrow, and bone tissues, activate the phagocytic, metabolic, and degradative processes to remove immune complexes originating from microorganisms, abnormal and aged cells, and NPs (Van Furth et al. 1972). The NPs in blood circulation are mainly removed in the liver and spleen. Nevertheless, when NPs are present in large quantities in the bloodstream, the liver and spleen eliminate only a fraction of the NPs while the others accumulate in tissues rich in macrophages, such as the lungs (Tavares et al. 2017). The recognition by macrophages and phagocytosis is initiated by opsonization; opsonins such as immunoglobulins and complementary proteins encompass the surface of NPs; thereafter, the phagocytotic activity commences (Xiang et al. 2012). The phagocytes ingest materials, including NPs, and form membrane-bound vesicles known as phagosomes. Later, the phagosomes make contact with lysosomes, and the NPs are degraded at acidic pH by hydrolytic enzymes in the lysosomal lumen (Uribe-Querol and Rosales 2017). The interaction between NPs and immune cells largely affects the pharmacokinetic fate of NPs in systemic circulation, ultimately causing selective accumulation at the disease site and toxicity.

Rigorous efforts have been made to determine the optimal physicochemical properties of NPs, such as size, shape, surface charge, and elasticity, and in turn result in improved pharmaceutical and pharmacokinetic functions of NPs by bypassing RES (Masserini 2013; Wang et al. 2015). For instance, the size of NPs can be controlled to avoid being easily recognized as foreign agents by immune cells. Accordingly, they exhibit prolonged blood circulation

(Behzadi et al. 2017; Ventola 2017). The size of NPs also affects their permeation into cells at pathologic sites. Recent studies have demonstrated that the geometrical shape of NPs governs the receptor-mediated cellular uptake pathways. Spherical NPs have a limited number of binding sites for receptors in cell membranes while non-spherical NPs allow multivalent interactions between NPs and cell surface receptors (Pada et al. 2019). The surface charge of NPs is highly correlated with their biological performance, including solubility, biodistribution, stability, cellular uptake, and cytotoxicity. Many cells have negative membrane potential (Alberts 2002). In addition, cells should undergo strong electrostatic interactions with cationic NPs. However, they are known to cause serious perturbation of the cell membrane and induce cytotoxicity (Jeon et al. 2018). Additionally, they adsorb plasma proteins and are rapidly removed from the systemic circulation by the RES. NPs with slightly negative charges are preferred because of their weak interactions with plasma proteins (Wang et al. 2016; Yu et al. 2019). Recent studies have focused on the elasticity of NPs. Optimization of the NP elasticity is a viable strategy for improving pharmacokinetic functionality, such as circulation time, immune response, and target efficiency. For example, soft NPs exhibit a decrease in the interaction with immune cells and are not easily eliminated by the RES. The resulting increase in the blood circulation time of soft NPs is expected to enhance their prospects of arriving at the pathologic site (Alexander et al. 2015; Anselmo et al. 2015; Guo et al. 2018a; Key et al. 2015).

As demonstrated in Fig. 1, we suggest that without sophisticated chemical modification, the modulation of physical parameters such as size, shape, surface charge, and elasticity of NPs change the fate of NPs in terms of cellular internalization and intracellular trafficking of NPs. Despite the vast number of investigations, understanding the interdependent role of each physical parameter on the pharmacokinetic functionality of NPs remains a challenge. In this review, we sought to discuss strategies to optimize the physical properties of NPs to enhance their pharmaceutical and pharmacokinetic functions. In addition, we aimed to emphasize the importance of NP elasticity during the development of effective drug delivery systems.

Size

The size of NPs is important in drug delivery. Not only is the activation of the immune response dependent on the size of NPs, but also the modulation of the pharmacokinetic functions including cell uptake, systemic circulation half-life, and the biodistribution of NPs, is significantly dependent on this feature. Unlike microparticles, NPs are not easily removed by the RES because of their small size.

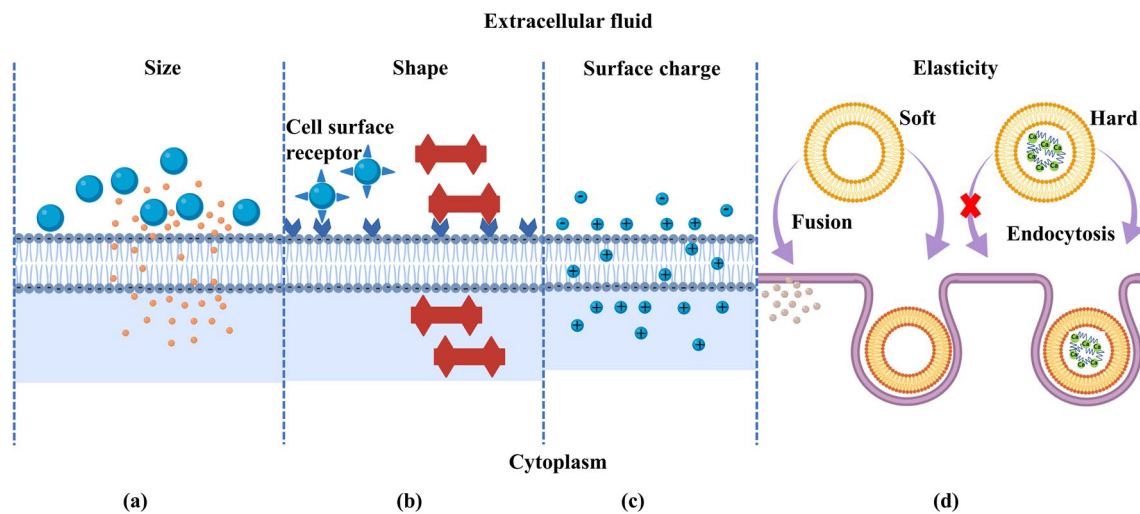


Fig. 1 Cell uptake affected by the physical parameters of nanoparticles: size (a), shape (b), surface charge (c), and elasticity (d)

As a result, they display relatively prolonged systemic circulation. Although the immune response triggered by drug delivery vehicles did not linearly depend on their size, the small size of the NPs is beneficial in the prevention of an interaction between NPs and the immune system (Liu et al. 2017). However, small NPs less than 5 nm in diameter are rapidly removed through renal clearance (Choi et al. 2007). Numerous studies have suggested that NPs with a size of 30–50 nm exhibit efficient cell uptake due to an increase in specific surface area and membrane-wrapping process (Lu et al. 2009). However, NPs with a diameter of less than 100 nm carry only a limited payload of therapeutic agents. Large NPs with diameters from 100 to 200 nm are required to deliver a sufficient amount of drugs to disease sites (Su et al. 2015). Microparticles of a few micrometers appeared to be advantageous because of their large drug-loading capacity but were easily filtered by the RES (Nagayama et al. 2007). The size of NPs also influences the pathway whereby NPs enter into cells. NPs 30–200 nm in diameter undergo intracellular incorporation via clathrin- or caveolin-dependent endocytosis (Rejman et al. 2004; Saw et al. 2018). However, the phagocytosis process is reported to be a major pathway whereby larger NPs with a size of 250 to 3000 nm are internalized into cells (Hillaireau and Couvreur 2009). It is important to strike a balance between both the risks and the benefits attributed to the size of NPs when determining the ultimate size of NPs for use as innovative vehicles with advanced pharmacokinetic functions.

The size of NPs plays a critical role in their blood circulation half-life and biodistribution under physiological conditions, such as hepatic filtration, extravasation, tissue diffusion, and kidney excretion. Renal clearance of intravascular components involves glomerular filtration, tubular secretion, and subsequent clearance of the molecules through urinary

secretion (Mangan et al. 2018). The glomerular capillary walls have a physiologic pore size of 4.5–5 nm (Ohlson et al. 2001). Thus, NPs with sizes less than 6 nm are efficiently filtered while those larger than 8 nm cannot be cleared by glomerular filtration. For example, Choi et al. reported that quantum dots with sizes of 4.36–5.52 nm exhibited renal clearance, whereas 8.65 nm quantum dots did not show renal filtration but uptake in the RES (Choi et al. 2007). The particles that are not filtered during renal clearance are excreted through the hepatic system. One of the main functions of the liver is to capture and eliminate foreign substances, including viruses and NPs (Choi et al. 2007). NPs with sizes of 10–20 nm are rapidly eliminated by the liver.

Many studies have focused on whether the size of NPs affects the circulation half-life and biodistribution. Talamini et al. reported that gold NPs with a size of 10 nm displays an increase in blood circulation time and a decrease in accumulation in the liver and spleen compared to 20 nm gold NPs (Talamini et al. 2017). Interestingly, 50 nm gold NPs displayed a dynamic behavior in blood circulation; the blood circulation time decreased during the first 24 h after the administration but later increased over 120 h. These findings indicated that the 50 nm NPs are easily internalized into cells while the 10 nm NPs escaped from the filter organs, passing through the endothelial cells and returning to circulation. Sonavane et al. also reported that small gold NPs (15 and 50 nm) have longer circulation times than gold NPs of 100 and 200 nm (Sonavane et al. 2008). Notably, these small gold NPs could penetrate the blood–brain barrier. The large gold NPs (100 and 200 nm) not only showed a short circulation half-life but also a high accumulation in the liver and spleen. The adsorption of serum proteins on NPs is considered to be one of the major parameters affecting the blood circulation time of NPs. Similarly, Nagayama

et al. reported a dramatic increase in the hepatic uptake of NPs when incubated with serum proteins (Nagayama et al. 2007). The adsorption of serum proteins on the surface of NPs is considered to induce an increase in opsonin-mediated uptake by Kupffer cells. Fang et al. reported that 80 nm poly methoxypolyethyleneglycol cyanoacrylate-co-n-hexadecyl cyanoacrylate (PEG-PHDCA) NPs caused a decrease in protein adsorption and phagocytic uptake compared to 170 and 240 nm PEG-PHDCA NPs (Fang et al. 2006). Consequently, the blood clearance of 80 nm NPs was two times slower than that of the 170 and 240 nm NPs.

Size governs the accumulation and penetration of NPs at tumor sites. The accumulation and distribution of NPs in tumors are altered by their residence time, local concentration gradient, and penetration depth. An increase in the size of NPs interferes with permeability in blood vasculatures. With passive targeting, the NPs accumulate at the tumor site by the enhanced permeation and retention effect. NPs with sizes of 30–200 nm are known to exhibit efficient tumor accumulation (Kobayashi et al. 2013; Miao and Huang 2015). Cabral et al. performed a comparative study to evaluate the accumulation efficiency of polymeric micelles with diameters of 30, 50, 70, and 100 nm in both highly and poorly permeable tumors (Cabral et al. 2011). They found that although all NPs penetrated the highly permeable tumors, only the micelles of 30 nm efficiently penetrated the poorly permeable pancreatic tumors to display an antitumor effect. These researchers also suggested that NPs smaller than 50 nm can penetrate poorly permeable hypovascular tumors. Perry et al. investigated the effect of size on the passive targeting of four different tumor models using hydrogel particle replication in non-wetting template (PRINT) particles of different sizes (55 × 60 nm, 80 × 180 nm, and 80 × 320 nm (Perry et al. 2017). These researchers included tumor models of SKOV3 human ovarian cells, 344SQ murine non-small cell lung cancer (NSCLC) cells, A549 human NSCLC cells, and A431 human epidermoid cancer cells. Based on their findings, the 55 × 60 nm particles preferentially accumulated in primary tumors and metastatic sites instead of healthy tissues while the 80 × 320 nm particles were mainly distributed in the regions close to blood vessels. Tchoryk et al. investigated the penetration of poly(styrene) NPs of 30, 50, and 100 nm in HCT-116 colorectal cancer spheroids (Tchoryk et al. 2019). Their results showed that the small NPs (30 and 50 nm) penetrated the core of ~80% of HCT-116 spheroids, whereas the 100 nm NPs were strongly associated with the periphery of spheroids without significant penetration. Tumor microenvironments, including the dense network of the extracellular matrix, often serve as physical barriers for NPs to penetrate deep regions of the tumor; small NPs penetrate more efficiently.

Due to the multi-faceted effects of size on various pharmacokinetic functions of NPs, a question arose: what size of NPs is desirable for using them as drug delivery vehicles. Recently, the so-called novel size-adjustable NPs have been suggested as an innovative alternative to resolve these issues. Cun et al. fabricated a smart-size-switchable nanoplatform by conjugating small dendrigraft poly-L-lysine (DGL) to poly(ethylene glycol)–poly(caprolactone)-micelles through a matrix metalloproteinase 2 (MMP-2)-sensitive peptide (Cun et al. 2018). After extravasation, smart NPs with an initial size of 100 nm swiftly released small 30 nm NPs in response to MMP-2 in the tumor microenvironment. By switching the size of NPs in the target sites, they achieved a significant increase in the penetration and anticancer efficacy in metastatic breast cancer cells (4T1) in vivo.

Rigorous studies have been conducted to evaluate the size-dependent uptake of NPs in different cell types. Saw et al. investigated the intracellular uptake, localization, and photothermal anticancer efficacy in breast cancer cells by fabricating cystine/citric acid-coated confeito-like gold NPs (confeito-AuNPs) of five different sizes: 30, 60, 80, and 100 nm (Saw et al. 2018). They found that the confeito-AuNPs of 30 nm had the highest cellular uptake via clathrin- and caveolae-mediated endocytosis while the other confeito-AuNPs utilized only clathrin-mediated endocytosis. Moreover, the confeito-AuNPs of 30 nm exhibited the highest photothermal cytotoxicity due to the high surface area relative to their total mass and the enhanced interaction between NPs and light. Similarly, Qian et al. demonstrated that phenylboronic acid-decorated soy protein NPs (30 nm, diameter) showed high cell uptake and cytotoxicity in HepG2 cells compared to their counterparts (50 and 150 nm) (Qian et al. 2019). Interestingly, to examine the effect of size on cellular uptake, a reductionist approach was adopted to minimize other physiochemical factors except the size of NPs. In these studies, co-exposure of NPs with different sizes was employed instead of the common single exposure. Li et al. reported that the co-exposure of large silica NPs with sizes of 50, 100, and 150 nm accelerated the uptake of small 50 nm silica NPs by HeLa cells (Li et al. 2019). The large silica NPs promoted the uptake of the small NPs while the small NPs inhibited the internalization of the large NPs. Although a clear mechanism has not been found to explain the interplay between NPs of different sizes on cellular uptake, it is postulated that the small silica NPs easily attach to the cell membranes because of their fast diffusion rate and competitively inhibit bigger silica NPs from adhering to the membranes (Sun et al. 2017). It has also been suggested that the attachment of bigger silica NPs to the cell membrane triggers the clathrin endocytosis machinery and thus enhances the internalization of the smaller silica NPs attached to cell membranes (Lesniak et al. 2013).

We learned that the size of NPs strongly affects different aspects of their pharmacokinetic behavior, including drug-loading capacity, cell uptake efficiency, intracellular trafficking, cell internalization pathways, systemic circulation time, excretion routes, tissue distribution, and tumor accumulation. Nevertheless, several complicated issues exist in determining the optimal size of NPs, leading to improvements in pharmacokinetic functions and drug efficacy. NPs with sizes of 100–200 nm, including microparticles, are beneficial due to their large drug-loading capacity. However, these large particles undergo active opsonization, easily trigger immune responses, rapidly accumulate in the liver and spleen, and thus display poor systemic circulation. In addition, restrictions in the cell internalization pathways were reported for these big particles; clathrin-mediated endocytosis for NPs of ~100 nm and phagocytosis of much larger particles (250–3000 nm in size) were recognized. However, there are obstacles to the use of small NPs with a size of less than 5 nm; this is not only because of their small loading capacity but also because of their rapid rate of renal clearance. Nevertheless, many studies revealed that compared to their larger counterparts, the small NPs were advantageous based on several aspects, including low immunogenicity, freedom for cell internalization pathways including caveolin-dependent pathways, long systemic circulation, and easy penetration and accumulation in the tumor. NPs of 30–200 nm have

often been used in many studies because of their high uptake efficiency and high tumor accumulation. Overall, it is evident that a smart choice must be made to determine a desirable size of NPs by considering the pros and cons regarding the drug-loading capacity, immune response, circulation time, and cell uptake.

Shape

A wide spectrum of nanomaterials, including liposomes, micelles, dendrimers, and metal NPs, have been employed as drug delivery systems. Although spherical or near-spherical NPs are most commonly used, recent advances in nano-engineering technology have instigated rigorous studies to determine whether the therapeutic efficacy can be improved by modulating the shape of NPs, as summarized in Table 1.

The shape of NPs dictates their ability to interact with cell membranes. Although spherical NPs provide limited binding sites for cell receptors, non-spherical NPs allow multivalent interactions with cell surface receptors, as shown in Fig. 1 (Agarwal et al. 2013). Non-spherical NPs exhibit efficient cell uptake by leveraging internalization pathways compared to their spherical counterparts (Bandyopadhyay et al. 2018; Shao et al. 2017; Zhang et al. 2019; Zheng et al. 2018). For example, Zheng et al. reported an increase in the uptake

Table 1 Pharmacokinetic improvements by non-spherical NPs compared to their spherical counterparts

| Formulation | Shape | In vitro findings | In vivo findings | References |
|---------------|-----------------------------|---|--|-----------------------------|
| Silica | Rod | High uptake in Caco-2 cells | High oral bioavailability | (Zheng et al. 2018) |
| | Rod | High uptake in MDA-MB231 Delayed drug release | | (Pada et al. 2019) |
| | Rod (AR = 4) | High uptake in HepG2 and HL-7702 | High accumulation in tumor | (Shao et al. 2017) |
| Gold | Rod (AR = 1.6) | High uptake and cytotoxicity in glioblastoma-astrocytoma cells | | (Bandyopadhyay et al. 2018) |
| Micelles | Filomicelle ($l = 180$ nm) | High uptake in Hela cells | Long blood circulation High accumulation in tumor | (Ke et al. 2019) |
| Polymer | Cylinder ($l = 203$ nm) | High uptake in A549 cells, SH-SY5Y cells and HUVECs | | (Zhang et al. 2019) |
| | Rod | High uptake in RBE4 endothelial cells | Specific accumulation in the lungs and brain | (Kolhar et al. 2013) |
| | Rod | High uptake in 4T1 cells Low uptake in RAW 246.7 macrophages | Long blood circulation High accumulation in tumor High antitumor efficacy | (Zhang et al. 2016b) |
| Dendrimer | Sheet | High uptake in 4T1 cells | Enhanced tumor accumulation High antitumor efficacy | (Guo et al. 2018b) |
| Nucleoprotein | Rod | | AR = 3.5: efficient passive tumor homing behavior ex vivo AR = 7: efficient tumor targeting in vivo | (Shukla et al. 2015) |

AR Aspect ratio, A549 human alveolar adenocarcinoma cells, Caco-2 colorectal adenocarcinoma cells, HepG2 human hepatocellular carcinoma cells, HL-7702 human hepatic embryo cells, HUVECs human umbilical vein endothelial cells, l length, SH-SY5Y human neuroblastoma cells, SPNPs spherical polymer nanoparticles, 4T1 murine mammary carcinoma cells

of mesoporous silica nanorods (MSNPs) in human epithelial colorectal adenocarcinoma (Caco-2) cells *in vitro* with respect to their spherical counterparts (Zheng et al. 2018). The MSNPs were internalized via the caveolae-mediated pathway while spherical NPs entered cells through clathrin-mediated endocytosis. Similar findings were reported in a study that investigated the interaction between magnetic mesoporous silica NPs (M-MSNPs) and human hepatocellular carcinoma cells (HepG2) and human hepatic embryo cells (HL-7702) (Shao et al. 2017). M-MSNPs with three different shapes—spheres with an aspect ratio (AR) of 1 and nanorods with AR=2 and 4—were synthesized. They showed that the long nanorods (AR=4) were most easily internalized by HepG2 and HL-7702 cells, and their internalization route was identified as macropinocytosis. In this study, the spheres and short nanorods were mainly internalized via the clathrin-mediated pathway. A similar study using gold NPs was performed on glioblastoma-astrocytoma cells (Bandyopadhyay et al. 2018). Gold NPs with five different shapes—nanorods (AR=2.8), bipyramids (AR=2.4), nanorods (AR=1.6), tetrahedra (AR=1.4), and spheres (AR=1)—were fabricated. They found that nanorods (AR=1.6) exhibited the highest cellular uptake and tumor cytotoxicity. Their uptake pathways include both receptor-mediated endocytosis and macropinocytosis. Unlike in the studies by Shao et al. the longest nanorods (AR=2.8) did not show the most efficient cell uptake. However, the nanorods were observed to be superior to the spherical gold NPs in terms of cell uptake efficiency. Ke et al. evaluated the uptake of ~2.5 μm (long), ~180 nm (short), and ~40 nm (sphere) filomicelles by HeLa cells (Ke et al. 2019). For comparative analysis, the cross-sectional diameters of filomicelles were kept constant at ~40 nm. As a result, they found that the short filomicelles had the highest cellular uptake due to the abundant interaction areas with the cell membranes relative to the spherical micelles. Although long filomicelles offered a stronger interaction with the cell membranes, the long structure induced steric hindrance that inhibited cellular internalization. They also reported that short and spherical micelles were internalized via clathrin- and caveolae-mediated pathways. The polymeric NPs were found to display consistent results. Zhang et al. reported that cylindrical polymer brushes (CPBs) of ~203 nm in length and ~17 nm in diameter showed higher uptake than spherical polymer NPs (SPNPs) of ~45 nm in diameter (Zhang et al. 2019). Different cell lines were investigated, including human alveolar adenocarcinoma cells (A549), human neuroblastoma SH-SY5Y cells, and human umbilical vein endothelial cells (HUVECs). The enhanced cellular uptake of the CPBs is due to their long and flexible morphology that provides larger contact areas with the cell membranes, leading to stronger interactions and adhesion with the cell membranes. Noticeably, they found that the internalization

pathways of polymeric NPs varied depending on not only the shapes, but also the cell lines. In A549 cells, the CPBs were internalized via clathrin-mediated endocytosis while SPNPs were internalized through caveolae-mediated endocytosis. In SH-SY5Y cells, both CPBs and SPNPs were internalized via clathrin-mediated endocytosis. In HUVECs, the main endocytic pathway for both NPs was micropinocytosis.

Additionally, the rod-shaped NPs were advantageous for targeting the endothelium at sites of inflammation. This is because they sustain hemodynamic forces that tend to detach NPs from the endothelium. Kolhar et al. fabricated polystyrene nanospheres with diameters of 200 nm and nanorods of 501 nm in length and 123.6 nm in diameter (Kolhar et al. 2013). The NPs were coated with either anti-ovalbumin antibody (OVA-mAb) or anti-intracellular adhesion molecule-1 antibody (ICAM-mAb) via physical adsorption. They evaluated specific interactions between the NPs and the walls of the synthetic microvascular networks coated with either OVA or laden with rat brain endothelial (RBE4) cells under the blood flow. The ICAM-mAb-coated nanorods were found to be internalized in the RBE4 cells to a much greater extent than the ICAM-mAb-coated spheres. ICAM-mAb-coated nanorods also exhibited the highest attachment to the endothelial monolayer under flow conditions *in vitro*. The enhanced avidity and specificity of the nanorods were ascribed to multivalent interactions that facilitate adhesion. Importantly, NPs with a high AR display an increase in their specific interactions and a decrease in nonspecific attachments to their targets compared to their spherical counterparts.

Studies have also shown that non-spherical NPs tend to delay drug release due to their uniqueness in porous networks. Pada et al. demonstrated that mesoporous silica nanorods coated with polydopamine and polyethylene imine-PEG had better cellular uptake and delayed drug release compared to spherical NPs (Pada et al. 2019). The nanorods had the lateral and helical alignments of their porous networks, in contrast to the radial alignments of the nanospheres, which are responsible for a prolonged diffusion path for the encapsulated drug molecules. The delayed drug release of the nanorods extended the duration of action of the drug molecules. Thus, the shape of NPs as drug delivery vehicles is one of the important design parameters for controlling their drug release profiles.

Moreover, non-spherical NPs exhibit a prolonged circulation time in the blood because of their ability to evade biological barriers such as RES and blood filtration (Guo et al. 2018c; Ke et al. 2019; Shukla et al. 2015; Zhang et al. 2016a). Zhang et al. also reported that the rod-shaped particles showed high uptake in 4T1 cells, displaying a three-fold longer blood circulation time than the spherical particles due to the difference in macrophage uptake (Zhang et al. 2016b). For the filomicelles mentioned earlier, short

filomicelles with a length of ~ 180 nm had a longer blood circulation half-life of 17.8 h than the spherical micelles (14.4 h) (Ke et al. 2019). However, long filomicelles with a length of ~ 2.5 μm were rapidly removed by the RES and exhibited a short blood circulation time in vivo with a circulation half-life of 9.7 h. The extremely lengthy filomicelles were postulated to be inferior to spherical micelles due to steric hindrance. It is interesting that the short filomicelles showed increases not only in cell uptake but also in blood circulation time. However, some experimental results have warned against our hasty inference that the non-spherical NPs showing better uptake efficiency have a longer blood circulation time. CPBs, which showed an increase in cell uptake, were phagocytosed 2.5 times more rapidly by RAW264.7 macrophages than their spherical counterparts (Zhang et al. 2019). Instead, the spherical NPs exhibited a longer circulation half-life (~6.2 h) than CPBs (~4.6 h) in that study.

According to numerous in vivo studies, the shape of NPs is also known to affect their biodistribution as well as blood circulation time. Many studies have suggested that rod-shaped NPs exhibit a decrease in liver uptake and renal excretion in vivo. Shao et al. reported that while spherical M-MSNPs were significantly accumulated in the liver, spleen, and kidneys, long-rod NPs with AR = 4 were only retained in the spleen (Shao et al. 2017). Huang et al. also found that long-rod NPs with AR = 5 were retained in the spleen after intravenous administration while the short-rod MSNPs with AR = 1.5 were easily trapped in the liver (Huang et al. 2011). However, an increase in AR did not guarantee escape from liver uptake and renal filtration. Zhang et al. reported that CPBs ~ 203 nm in length and ~ 17 nm in diameter had a more rapid hepatobiliary and renal excretion than the SPNPs with a diameter of ~ 45 nm (Zhang et al. 2019). Ke et al. also indicated that long filomicelles with a length of ~ 2.5 μm exhibited both a high clearance by the RES and a high retention in the liver and spleen (Ke et al. 2019). Similar findings were reported for nucleoprotein-based nanorods fabricated from tobacco mosaic virus protein. The long nanorods with AR = 16.5 were rapidly cleared by the RES and accumulated in the liver and spleen compared to other nanorods with AR = 3.5 and 7, while the short NPs with AR = 3.5 had longer circulation times (Shukla et al. 2015). Li et al. reported that although the rod-shaped MSNPs had decreased renal excretion and liver distribution compared to their spherical counterparts after oral administration, in vitro studies using simulated intestine and gastric fluids showed that their degradation rates and bioavailability were reduced (Li et al. 2015). Indeed, the degradation of NPs was shape dependent. With the increase in AR, the degradation rate decreased, and thus, the nanospheres exhibited the highest degradation rate in vitro. These complex effects of the

shape of NPs on biodistribution highlighted the need to engineer the shape of NPs.

To date, we have learned that a simple change in the shape of NPs could result in improved pharmacokinetic functions. Remarkably, these improvements, which were derived by modulating the shape of NPs, led to enhanced tumor penetration and accumulation, which is essential for elevated drug efficacy. For instance, deep penetration into multicellular spheroids was achieved by ~ 203 nm CPBs, showing high cellular uptake in vitro (Zhang et al. 2019). The enhanced flexibility of CPBs allowed them to alter the spatial conformation of the tumor microenvironments. Similar improvements in tumor spheroid penetration were reported for short filomicelles with a length of ~ 180 nm compared to spherical micelles (Ke et al. 2019). Moreover, in vivo experiments have reported the high antitumor efficacy of short filomicelles. In vivo studies have reported similar results. The fiber rods exhibited lower uptake by macrophages, leading to three times longer blood circulation time and four times higher accumulation in mammary tumors than microspheres after intravenous administration (Zhang et al. 2016a). A comparative study using an amphiphilic PAMAM-b-OEG codendrimer also revealed the better antitumor efficacy of non-spherical NPs than that of nanospheres, which is attributed to an increase in the blood circulation time and the tumor penetration of the nanosheets (Guo et al. 2018b). Many experimental findings support the enhanced tumor penetration and antitumor efficacy of non-spherical NPs. However, whether the use of nanorods with high AR is beneficial for improving drug efficacy remains unclear. In a similar study conducted by Shukla et al., they found that PEGylated nanorods with the lowest AR (AR = 3.5) exhibited excellent passive tumor-homing behavior due to their efficient diffusion ability (Shukla et al. 2015). However, nanorods with the medium AR (AR = 7) showed efficient tumor targeting, which was attributed to the enhanced balance between infusibility and ligand-receptor interactions.

Overall, the shape of NPs dictates the interactions between NPs and target cells. Non-spherical NPs with a low AR, such as rods and sheets, have improved cell uptake and prolonged blood circulation time due to their reduced clearance by the RES. Moreover, non-spherical NPs have advantages in tumor penetration and accumulation because they offset the hemodynamic forces that tend to detach the NPs from the endothelium. Thus, it is worthwhile to design the shape of NPs to improve the pharmacokinetics of NP therapeutics.

Surface charge

The surface charge of NPs, represented by zeta potential, affects the phagocytic uptake of NPs and thus affects the pharmacokinetics and biodistribution of NPs (Zhang et al.

2008). The cells exhibit a slight negative potential difference across their plasma membranes. The membrane potential varies from cell to cell, ranging from -90 mV to -20 mV (Alberts B 2002; Yang and Brackenbury 2013). Neurons are known to exhibit the most distinctive potential difference. The surface charge of NPs and cell membrane potential regulate cellular internalization, localization, and biological functions of NPs (Arvizo et al. 2010). Importantly, the surface charge of NPs governs the electrostatic interactions between NPs and surrounding proteins, thereby affecting the blood circulation time and the pharmacokinetics of NPs, as summarized in Table 2.

Some studies have demonstrated that cationic NPs are efficiently internalized into cells due to their electrostatic interactions with the cell membranes that had a negative potential. For instance, cationic fluorophore-conjugated polystyrene NPs had a high internalization efficiency in both phagocytic differentiated (THP-1) and non-phagocytic (A549) cells compared to the neutral and anionic NPs (Jeon et al. 2018). Similarly, Kang and coworkers showed that cationic liposomes ($+43$ mV) exhibited high uptake in glioblastoma cells (U87MG) and fibroblasts (NIH/3T3) compared to anionic (-15 mV) and neutral (-5 mV) liposomes (Kang et al. 2017). A further study showed that cationic liposomes were internalized into glioblastoma cells through the macropinocytosis pathways while the neutral liposomes were internalized via caveolae-mediated endocytosis. However, in fibroblasts, all liposomes were internalized

via clathrin-mediated endocytosis. Song et al. also demonstrated that cationic cellulose-based NPs encapsulating lysozyme and bovine serum albumin proteins showed high uptake efficiency in colorectal adenocarcinoma cells (Caco-2) (Song and Chen 2015). The strong surface charge and large surface-to-volume ratio of cellulose NPs enhanced cellular uptake efficiency. Similarly, Zhang et al. showed that the cell uptake of NaYF₄: Yb³⁺, Er³⁺ up-conversion NPs strongly depends on the surface charge; the cationic NPs exhibited high uptake efficiency in HeLa cells (Zhang et al. 2018). A further study of the shape of NPs showed that 2-D hexagonal structures had higher cellular internalization efficiency than their 3-D counterparts. Notably, when the size of NPs increases, the role of surface charge on cellular internalization is weakened and the shape becomes a major factor driving the cellular internalization process. An interesting study was performed on cationic gold NPs. Arvizo et al. reported that cationic gold NPs showing high uptake induced membrane depolarization in ovarian cancer cells, human bronchial epithelial cells, and human airway smooth muscle cells (Arvizo et al. 2010). Membrane depolarization by cationic gold NPs led to an increase in the intracellular calcium concentration by stimulating membrane calcium influx and endoplasmic reticulum calcium release.

As summarized in Table 2, cationic NPs showed enhanced cellular uptake in diverse types of cells, including cancer cells and macrophages. Nevertheless, both cationic and anionic NPs undergo active opsonization due to the

Table 2 Effect of surface charge on the pharmacokinetic functions of NPs in vitro and in vivo

| Charge | Formulation | In vitro and In vivo findings | Referenes |
|-----------|--|---|---|
| Cationic | Gold | High uptake in CP70, A2780, BEC, and ASM cells Significant membrane depolarization | (Arvizo et al. 2010) |
| | Polymer | High uptake in THP-1 macrophages and non-phagocytic A549 Cells | (Jeon et al. 2018) |
| | | High uptake in A549, TRAMP-C1 and MCF-7 and high antitumor activity | (Meng et al. 2016), (Hung et al. 2016) |
| | Liposomes | High extravasation and accumulation in TRAMP-C1 tumor, | (Hung et al. 2016) |
| | | High uptake in U87MG and NIH/3T3 | (Kang et al. 2017) |
| | | High uptake in Caco-2 cells | (Song and Chen 2015) |
| Inorganic | High uptake in HeLa cells | (Zhang et al. 2018) | |
| Anionic | Quantum dots | High uptake in MDA-MB231 and RAW 264.7 macrophages Long blood circulation | (Liu et al. 2015) |
| | Polymer | Low cytotoxicity in L929 fibroblasts | (Shao et al. 2015) |
| | | Long circulation time | (He et al. 2010) |
| | | High accumulation in H-22 tumors | |
| | Micelle | Low uptake in RAW 264.7 macrophages | (Xiao et al. 2011) |
| | | Long circulation time High accumulation in SKOV-3 tumor | |
| Pectin | Long circulation time | (Verma and Kumar 2013) | |
| Gold | Long circulation time High accumulation in U14 tumors | (Wang et al. 2016) | |

A2780, CP70 ovarian cancer cells, A549 adenocarcinomic human alveolar basal epithelial cells, ASM human airway smooth muscle cells, BEC human bronchial epithelial cells, Caco-2 colorectal adenocarcinoma cells, NIH/3T3 embryonic fibroblasts, U87MG human glioblastoma cells

strong electrostatic adsorption of proteins on the surface of NPs in the bloodstream. Instead, neutral NPs can resist protein adsorption due to the lack of electrostatic interactions, avoid filtration by the mononuclear phagocyte system, and thus achieve low clearance and prolonged blood circulation time compared to charged particles. Notably, cationic NPs have a high affinity for adsorbing plasma proteins, which increases their hydrodynamic size, leading to rapid clearance and subsequent accumulation in the lungs. Moreover, the strong ionic interactions between cationic NPs and the negatively charged cell membrane resulted in an accumulation of the NPs in the lung and kidney. Xiao et al. reported an increase in the uptake of charged micelles by the RAW 264.7 murine macrophages due to active opsonization in mouse serum (Xiao et al. 2011). Further *in vivo* studies showed that NPs mainly accumulated in the liver due to phagocytosis by macrophages (Kupffer cells). In contrast, NPs carrying slightly negative charges showed a decrease in liver accumulation and an increase in tumor uptake as a result of reduced clearance by the RES. An interesting study reported the enhanced bioavailability of cationic polymeric NPs administered via the oral route (Du et al. 2018). In that study, cationic NPs exhibited significant uptake both in Caco-2 cells *in vitro* and small intestinal epithelial cells *in vivo*, strongly interacted with both the epithelial surface and lamina propria, and thus accumulated in the small intestine. Subsequently, the NPs were transported via the mesenteric vessels to the liver through the hepatic portal vein and finally to the systemic circulation, resulting in significantly improved oral bioavailability. However, Verma et al. showed that a negative charge is more suitable for the passive delivery of drugs in the liver. They found that anionic pectin NPs exhibited prolonged plasma retention of paclitaxel with major accumulation in the liver via intravenous injection *in vivo* (Verma and Kumar 2013).

However, studies using quantum dots have reported results that are conflicting to other NPs in terms of the role of surface charge on cellular interactions. Some studies have reported preferential internalization of cationic NPs, while others have reported preferential uptake of anionic quantum dots. For instance, Liu et al. demonstrated that charged quantum dots (either positive or negative) exhibited higher internalization in breast cancer cells (MDA-MB-231) than their neutral counterparts. Surprisingly, the anionic NPs showed higher cellular uptake due to their high hydrophobicity than neutral and cationic NPs (Liu et al. 2015). A further study showed that all quantum dots were internalized into the cells predominantly via clathrin-mediated endocytosis. In addition, an intracellular transport study showed that the anionic quantum dots had high penetration ability and were accumulated in endosomes and lysosomes compared to neutral NPs localized in the cytoplasm and lysosomes. Moreover, the anionic and neutral NPs had a longer blood circulation time

than the cationic quantum dots and preferentially accumulated in the liver and spleen. Strikingly, the cationic quantum dots were accumulated in the kidney and brain, implicating that they could open the tight junctions around the capillaries in the brain. Tang et al. also demonstrated that cationic quantum dots were preferentially accumulated in the lungs while the anionic and PEGylated counterparts were accumulated in the liver (Tang et al. 2013). High doses of cationic quantum dots caused severe acute toxicity both *in vivo* and *in vitro* owing to pulmonary embolism. Nevertheless, PEGylated quantum dots significantly reduced chronic injury relative to either cationic or anionic quantum dots. Unlike other types of NPs, quantum dots display a unique dependence on systemic circulation time for their surface charge. Javidi et al. demonstrated that anionic quantum dots had a longer systemic circulation time than their cationic counterparts (Javidi et al. 2019).

Cytotoxicity and unexpected side effects were observed not only for quantum dots but also for other types of NPs. Strong charges were suggested to result in more severe outcomes caused by NPs. Shao et al. also demonstrated that cationic polymeric NPs caused significant cytotoxicity to L929 fibroblasts compared to anionic NPs (Shao et al. 2015). They reported that the strong charges of NPs exacerbate cytotoxicity. Under physiological conditions, the protein corona surrounding the cationic NPs weakens the interactions between NPs and the cell membranes. However, as the corona is decomposed in the lysosomes, the cationic NPs are more exposed. Furthermore, they strongly interact with lysosomal membranes and finally induce significant cytotoxicity. However, the interactions between the anionic NPs and biological membranes are inherently repulsive regardless of the corona formation as biological membranes, including lysosomal membranes, are also negatively charged.

Different studies have demonstrated that NPs with different surface charges display distinctive features in terms of tumor accumulation and penetration. For example, Meng et al. reported that cationic polymeric NPs encapsulating tetrandrine had a higher cellular uptake efficiency and excellent antitumor activity in A549 cells than anionic NPs. This finding was attributed to the enhanced adsorption of the cationic NPs to the cell membrane with anionic proteins, thereby facilitating uptake into the cytoplasmic compartments (Meng et al. 2016). Another study by Wang et al. demonstrated that anionic gold NPs had longer systemic circulation time, higher tumor uptake efficiency, and subsequently a stronger antitumor effect (54.3%) in murine cervix carcinoma U14 cells than their neutral (38.9%) and cationic (42.2%) counterparts (Wang et al. 2016). They indicated a decrease in nonspecific cellular uptake and the adsorption of plasma proteins of the anionic NPs in the phagocytic system as the main causes of the observed differences. He et al. also found that a slight negative charge of chitosan NPs exhibited

a long circulation time, thereby contributing to significant accumulation in the tumor relative to the cationic and anionic NPs (He et al. 2010).

Cationic NPs are known to exert electrostatic forces on cell membranes with negative potential and thus facilitate binding events with tumors. However, the neutral or slightly negative charges were found to be favorable for preventing nonspecific binding during circulation (Naguib et al. 2014). Novel NPs with switchable charges have been exploited to enhance the internalization of target tissues and therapeutic efficacy. Owing to the tumor microenvironments, smart moieties responding to external stimuli, including pH-responsive moieties, have been incorporated into this novel NP system. For instance, Hung et al. fabricated pH-responsive NPs consisting of hydrophobic poly(lactic-co-glycolic acid) PLGA cores coated with pH-responsive N-acetyl histidine-modified D- α -tocopheryl polyethylene glycol succinate (NACHis-TPGS) shells to deliver doxorubicin (DOX) into tumors (Hung et al. 2016). The NPs with an initial neutral charge turned into cationic NPs under acidic conditions, which solicit protonation of the imidazole group of the NACHis-TPGS segments. The resulting positive charge of NACHis-TPGS/PLGA NPs enhanced the delivery efficiency of DOX to TRAMP-C1 cells and MCF-7 cancer cells by 1.5 folds under acidic conditions *in vitro*. An *in vivo* biodistribution study also showed that the NACHis-TPGS/PLGA NPs were significantly accumulated in the tumor and actively penetrated the deep tumor under hypoxic conditions. As a result, the improved pharmacokinetic functions due to the switchable charges led to the successful inhibition of tumor growth and recurrence *in vivo*. Similar pH-responsive magnetic nanoparticles (MNPs), which can switch their surface charges from -13.8 mV to $+31$ mV, were fabricated (Shen et al. 2013a). At a physiological pH of 7.4, the pH-responsive NPs exhibited a surface charge of -13.8 mV and thus repelled the negatively charged cell membrane during blood circulation. Once the NPs were delivered to the tumor site, the acidic condition of the tumor turned the surface charge of NPs into a positive charge by removing galactose from the Schiff base and protonating the ϵ -amino groups in the lysine residue of NPs. Consequently, they successively achieved a significant increase in the uptake of NPs in epithelial carcinoma A549 cells through electrostatic interactions between the cationic NPs and the negatively charged cell membrane.

Generally, cationic NPs are efficiently internalized into cells due to electrostatic interactions with the negatively charged membrane. However, the high interaction of cationic NPs with opsonin proteins accelerates their rate of clearance from the bloodstream. The slightly negative charges of NPs are known to be beneficial for the extended blood circulation time owing to the reduced interactions with the RES. With the long blood circulation time, the NPs could reach the disease sites. Recently, novel NPs with switchable charges have

been suggested as an innovative alternative that can leverage the effect of the surface charge of NPs on pharmacokinetic functions for improved therapeutic efficacy.

Elasticity

Rigorous efforts have been made to determine whether the elasticity of NPs is a major physicochemical determinant affecting the pharmacokinetics and biodistribution of NPs. Elasticity represents the flexibility of a material under stress (e.g., shear, uniaxial, or bulk stresses). Many studies report that the elasticity of NPs affects the manner in which NPs interact with immune cells and organs (Anselmo et al. 2015; Hartmann et al. 2015; Key et al. 2015; Merkel et al. 2011; Mullner et al. 2015). To date, several techniques have been utilized to evaluate the elasticity of NPs, such as mechanical tester (Liu et al. 2012), rheometer (Anselmo et al. 2015), extrusion (Utreja et al. 2011), synchrotron X-ray diffraction (Ingham et al. 2010), scanning tunneling microscopy (Hazarika et al. 2014), and atomic force microscopy (AFM) (Takechi-Haraya et al. 2019). Among these techniques, AFM has been extensively used to evaluate the elasticity of NPs (Cui et al. 2013; Hartmann et al. 2015; Teschke and de Souza 2002; Zhang et al. 2015).

Because of the high spatial resolution (< 1 Å) and the high sensitivity in force detection (~ 1 pN), AFM has been used to evaluate the morphological and mechanical properties of NPs (Liang et al. 2004; Takechi-Haraya et al. 2018). For the elasticity measurements, the AFM probe was used to apply a precisely controlled force on the sample surface and yielded a force-distance curve (Brochu and Vermette 2008; Teschke and de Souza 2002). The obtained force-distance curves were analyzed using mathematical models, such as the Hertz model, to determine the elasticity (Young's modulus) of the sample (Bolean et al. 2017; Brochu and Vermette 2008). Further alterations to the Hertz model allowed quantification of both the elastic storage modulus and viscous loss modulus of the sample (Mahaffy et al. 2004). The frequency-dependent analysis facilitated the decomposition of the elastic modulus into loss and storage modulus (Mahaffy et al. 2004; Pi et al. 2000). The Hertz model was also expanded to determine the elastic moduli of very thin soft materials considering the boundary conditions of samples (Brochu and Vermette 2008; Mahaffy et al. 2004). Force-distance curves were often collected in a two-dimensional array over a defined area of the sample. The force-distance curves or force volume data were very useful for evaluating the spatial variations in elasticity. By analyzing the force volume, the entire map of the distribution of Young's moduli over the scanned area can be generated (Bastatas et al. 2012).

Table 3 summarizes how the elasticity of NPs affects cellular uptake and intracellular trafficking of NPs. Soft NPs

are reported to be internalized into cancer cells faster and to a greater extent than hard NPs (Guo et al. 2018a; Hartmann et al. 2015; Liu et al. 2012; Sun et al. 2015a). For instance, Liu et al. found that soft NPs (17 kPa) made of poly(2-hydroxyethyl methacrylate) (HEMA) hydrogel were more efficiently internalized into HepG2 cancer cells than the stiffer NPs (156 kPa) (Liu et al. 2012). Micropinocytosis was identified as a major route for the soft NPs to enter cells while stiffer NPs were internalized via caveolae- and clathrin-mediated endocytosis as well as macropinocytosis. The internalization of the stiffer NPs disturbed the cell morphology as well as the internal structures by the formation of vacuoles in the cell body. The hard NPs resulted in strong impedance of cell adhesion and interfered with the adjustment of the membrane structures during adhesion. Subsequently, these changes modulated the cell functions, including cell growth, migration, differentiation, survival, and tissue organization. Similarly, Hartmann et al. reported rapid internalization of soft polymeric capsules to the lysosomes of HeLa cells (Hartmann et al. 2015). Sun et al. demonstrated that soft hyaluronic acid capsules efficiently bind to HeLa cells compared to stiffer capsules (Sun et al. 2015a). It was postulated that when contact was made with the cell membrane, the soft capsules easily deformed their shape, resulting in a large contact area that facilitated their adhesion to the cell membrane. Some studies have suggested that the difference in the cellular uptake of soft and hard NPs results from the shift of the internalization pathway from fusion with a low energy dependence to endocytosis with a high energy dependence. Guo et al. also demonstrated that soft NPs were predominantly internalized via the fusion mechanism while the hard NPs underwent clathrin-mediated internalization. Thus, soft NPs with an elastic modulus of

45 kPa exhibited higher uptake by breast cancer cells (MDA-MB231 and MCF-7) and human mammary epithelial cells (MCF-10A) than the hard NPs with an elastic modulus of 19 MPa (Guo et al. 2018a). It is understandable that the fusion pathway is only allowed for NPs with low elastic moduli because they can quickly squeeze themselves within the cell membrane pores and thus require less energy. However, the uptake of the NPs into the cells by the endocytosis pathways requires high energy expenditures to bend the membrane, overcome the surface tension, and coat the pits. Therefore, fusion of the soft NPs within the cell membrane without endosome formation might be an efficient route for the intracellular delivery of therapeutic agents.

Nevertheless, some studies reported that the hard NPs exhibited high cellular uptake due to the lower energy consumption by the membranes in wrapping their surfaces than soft NPs (Anselmo et al. 2015; Sun et al. 2015b; Zhang et al. 2015). According to Sun et al. soft NPs undergo significant deformation during cell uptake before they are trapped within the cell membrane (Sun et al. 2015b). This deformation impedes their entry into the cells because of the high energy demand to overcome the bending energy required to complete their internalization. They reported that hard poly(lactic-co-glycolic acid) (PLGA)–lipid NPs with an elastic modulus of 1.2 GPa displayed significantly higher uptake by HeLa cells than the soft PLGA–lipid NPs with an elastic modulus of 0.76 GPa (Sun et al. 2015b). As a result, the hard NPs loaded with doxorubicin induced more cell death than their soft counterparts. Both the hard and soft NPs were internalized via clathrin-mediated endocytosis. Similarly, Zhang et al. demonstrated that hard lipid-monolayer polymeric NPs loaded with doxorubicin had higher uptake in HeLa cells, leading to an enhanced anticancer

Table 3 Uptake of soft NPs by different cells

| Formulation | Softness | Cells | References |
|---------------------------------|---------------------------|---------------------------|-------------------------|
| High uptake in cancer cells | | | |
| Polymer | 0.25 – 5 N/m | HeLa cells | (Hartmann et al. 2015) |
| | 610 – 1×10^7 kPa | MDA-MB231, SUM159 | (Alexander et al. 2015) |
| Hyaluronic acid | 7.6 – 28.9 N/m | HeLa cells | (Sun et al. 2015a) |
| Liposomes | 45 – 19,000 kPa | MDA-MB231, MCF-7, MCF-10A | (Guo et al. 2018a) |
| Low uptake in endothelial cells | | | |
| PEG-based hydrogel | 10 – 300 kPa | bEnd.3 | (Anselmo et al. 2015) |
| Polymer-lipid | N/A | HUVECs | (Zhang et al. 2015) |
| PLGA–lipid | 0.76 – 1.20 GPa | HUVECs | (Sun et al. 2015b) |
| Low uptake in macrophages | | | |
| Polymer-lipid | ~1.3 and 15 kPa | J774.A1 | (Key et al. 2015) |
| Polymer | N/A | RAW 264.7 | (Mullner et al. 2015) |
| | 610 – 1×10^7 kPa | J774.A.1 | (Alexander et al. 2015) |
| Micelles | N/A | THP-1 | (Geng et al. 2007) |

HUVECs human umbilical vein endothelial cells, PEG polyethylene glycol diacrylate, PLGA poly(lactic-co-glycolic acid)

effect, than soft NPs (Zhang et al. 2015). They explained that the soft NPs dissipated more energy at the lipid NP-cell interface and were thus less internalized by cancer cells than the hard NPs. Moreover, Anselmo et al. reported the high internalization efficiency of hard polyethylene glycol (PEG)-based hydrogel NPs with an elastic modulus of 3 MPa in 4T1 cancer cells as a result of the enhanced receptor-mediated endocytosis compared to the soft NPs with an elastic modulus of 10 kPa (Anselmo et al. 2015).

The endothelial cells line the interior surface of the blood and lymphatic vessels. Further, they act as a barrier between the vessel lumen and surrounding tissues, controlling the entry of foreign materials, including NPs. NPs of optimal formulation can permeate the endothelial barriers and deliver therapeutic agents to the intended target tissue. Some studies have shown that soft NPs are preferentially internalized by endothelial cells relative to hard NPs. Alexander et al. reported that soft cube-shaped TA/PVPON polymer capsules exhibited higher internalization in human microvascular endothelial cells because of the low energy demand for membrane deformation than hard capsules (Alexander et al. 2015). Nevertheless, other studies have demonstrated more efficient internalization of hard NPs than soft NPs (Anselmo et al. 2015; Sun et al. 2015b; Zhang et al. 2015). Their findings are due to the full wrapping of the hard NPs by the cell membrane and their efficient internalization into the endothelial cells. The soft NPs undergo deformation during internalization and *are trapped within the cell membrane*. For instance, Sun et al. reported that hard PLGA–lipid NPs with an elastic modulus of 1.2 GPa were efficiently internalized into HUVECs compared to soft PLGA–lipid NPs with an elastic modulus of 0.76 GPa (Sun et al. 2015b). Similar results were demonstrated by Zhang et al. that hard lipid-monolayer polymeric NPs loaded with doxorubicin had a higher uptake in HUVECs due to the enhanced cell-particle interaction, which induced significant cytotoxic effects, than their soft counterparts (Zhang et al. 2015). In addition, Anselmo et al. found that hard hydrogel NPs with an elastic modulus of 3 MPa showed efficient uptake in endothelial bEnd.3 cells owing to enhanced receptor-mediated endocytosis compared to soft NPs with an elastic modulus of 10 kPa (Anselmo et al. 2015). Although there have been equivocal reports regarding the role of elasticity on the uptake efficiency of NPs by endothelial cells (Alexander et al. 2015), many studies have shown enhanced internalization of the hard NPs by endothelial cells (Anselmo et al. 2015; Sun et al. 2015b; Zhang et al. 2015).

The mononuclear phagocyte system, reticuloendothelial system (RES), removes foreign substances from blood circulation. It includes monocytes of the blood and macrophages in the liver, spleen, bone marrow, and lung (Van Furth et al. 1972). The NPs in the systemic circulation are eliminated by RES. Many researchers have attempted to minimize the

interactions of NPs with monocytes and macrophages that eliminate the NPs from circulation by optimizing the elasticity of NPs, as shown in Table 3. Key et al. fabricated discoidal polymeric NPs (DPNPs) with different elastic moduli from ~ 1 to 15 kPa and evaluated their interactions with bone marrow-derived monocytes (Key et al. 2015). The soft DPNPs were found to be twice as internalized as the hard DPNPs. Moreover, the hard DPNPs were efficiently internalized by the J774.A1 macrophages three times faster than the soft DPNPs. The soft DPNPs could transiently deform their shape, squeeze through small orifices, such as circulating blood cells, ultimately resulting in decreased interactions with the RES. Hard hydrogel NPs with an elastic modulus of 3 MPa were also reported to be efficiently phagocytosed by the J774.A1 macrophages (i.e., 3.5 folds greater than the soft NPs with an elastic modulus of 10 kPa) (Anselmo et al. 2015). During phagocytosis, macrophages exert a force on NPs that is strong enough to deform the soft NPs; this may be responsible for the findings achieved. Due to the deformation, soft NPs become elongated or stretched in a direction parallel to the cell membrane. Consequently, the extent of phagocytosis decreases. In addition, an increase in the tension of the cell membrane that is required to sustain complete phagocytosis may contribute to a decrease in the extent of phagocytosis. Phagocytosis is known to decrease in proportion to the radius of curvature of spherical NPs (Champion and Mitragotri 2006; Herant et al. 2005). Furthermore, hard cube-shaped hydrogen-bonded tannic acid/poly(N-vinylpyrrolidone) (TA/PVPON) polymer capsules showed a higher uptake by the J774A.1 murine macrophages than the soft capsules (Alexander et al. 2015). These studies consistently reported that hard NPs are effectively internalized by macrophages compared to soft NPs, indicating the potential prolongation of the blood circulation time of soft NPs.

Importantly, the elastic properties of NPs affect the circulation half-life of NPs by minimizing their rapid clearance using immune-competent cells. Soft NPs persist in the bloodstream for a long time due to their reduced uptake by macrophage cells. Anselmo et al. reported that soft hydrogel NPs with an elastic modulus of 10 kPa exhibited longer circulation time (< 2 h), resulting in their accumulation in certain organs in vivo, than hard hydrogel NPs with an elastic modulus of 3 MPa (Anselmo et al. 2015). The reduced opsonization of soft NPs by the macrophage-hosting RES organs was considered to be a major cause. Similarly, soft DPNPs with an elastic modulus of ~ 1.3 kPa exhibited a longer circulation half-life (24 h) than the hard DPNPs with an elastic modulus of 15 kPa (Key et al. 2015). The hard NPs were rapidly removed from pulmonary microcirculation by Kupffer cells, *leading to significant accumulation in the liver and abdominal cavity at 6 h after administration*. Mullner et al. also reported that soft CPBs have a longer circulation

half-life (> 24 h) than their hard counterparts. The elasticity of anisotropic material was found to significantly influence the clearance and filtration of NPs in the blood (Mullner et al. 2015). Additionally, Merkel et al. conducted similar studies by fabricating mimicry red blood cell hydrogel microparticles (RBCMs) with an elastic modulus of 63.9, 39.6, 16.9, and 7.8 kPa (Merkel et al. 2011). The hard RBCMs with an elastic modulus of 63.9 kPa and 39.6 kPa were rapidly sequestered after administration and were accumulated in the lungs. However, the soft RBCMs with an elastic modulus of 16.9 kPa and 7.8 kPa avoided clearance by filtration in the lung; instead, they were accumulated in the spleen. Strikingly, the concentration of soft RBCMs in the lung and spleen decreased over time, revealing that the particles were not permanently trapped and might return to circulation. Consequently, the soft RBCMs with an elastic modulus of 7.8 kPa had the longest circulation half-life.

Furthermore, elastic properties play a critical role in biodistribution, including the selective accumulation of NP therapeutics in target organs. The long circulation time of NPs extended their duration of action and thus induced the accumulation of therapeutic agents at disease sites such as tumors (Guo et al. 2018a; Key et al. 2015; Zhang et al. 2015). The study that employed NPs with an elastic modulus of 45 kPa, 1.6 MPa, 13.8 MPa, and 19 MPa reported that soft NPs with an elastic modulus of 45 kPa exhibited significant tumor accumulation with a 1.3-, 1.9-, and 2.6-fold increase relative to the hard NPs with an elastic modulus of 1.6 MPa, 13.8 MPa, and 19 MPa, respectively (Guo et al. 2018a). Moreover, hard NPs with elastic moduli above 13.8 MPa were more accumulated in the liver than soft NPs with elastic moduli of 45 kPa and 1.6 MPa. Similar results have been reported where the long half-life (~24 h) of soft DPnPs with an elastic modulus of ~1.3 kPa facilitated their accumulation in the tumor (Key et al. 2015). The iron-loaded soft DPnPs efficiently targeted the malignant mass. Further, the accumulation of these DPnPs reached more than 15% ID/g at 3 h after administration in the presence of a magnetic field. However, studies have reported the superiority of hard NPs relative to soft NPs. For example, Zhang et al. demonstrated that the hard lipid-monolayer-shell NPs loaded with doxorubicin and combretastatin A-4 exhibited stronger tumor growth inhibition and higher targeting efficiency than the soft lipid-bilayer-shell NPs *in vivo* (Zhang et al. 2015). These results aligned with those from their *in vitro* studies where hard NPs were demonstrated to have strong interactions and adhesion to both HUVECs and HeLa cells.

Generally, the elastic modulus of NPs is an important parameter that modulates the pharmacokinetic behavior of NP therapeutics. Optimization of the elastic modulus has been shown to influence the interactions between NPs and various cells, circulation half-life, tumor targeting, and accumulation efficiency. Soft NPs were reported to be efficiently

internalized by cancer cells despite a lack of conclusion regarding the uptake efficiency of soft NPs in endothelial cells. Importantly, most *in vivo* and *in vitro* studies have demonstrated that soft NPs are less internalized by immune cells and exhibit longer circulation time than hard NPs. Nevertheless, some *in vitro* studies arrived at conclusions that opposed these findings.

Conclusion

NP drug delivery systems have garnered increased attention because they reduce drug toxicity, extend blood circulation half-life by reducing immunogenicity, and allow controlled drug release. NP systems also facilitate targeted and site-specific drug delivery. Despite these advantages, NPs have yet to achieve their full potential as drug delivery vehicles. NPs in systemic circulation are considered foreign substances and are rapidly cleared by the RES. Strikingly, the recognition of NPs in systemic circulation can be adjusted by controlling the physicochemical parameters of NPs. NPs with small sizes in the range of 30–200 nm are ideal candidates that balance several aspects of pharmacokinetic features, including cell uptake, recognition by the RES system, and physiological filtration in the kidney, liver, and spleen. In addition, elongated NPs were revealed to exhibit high cellular internalization through multivalent interactions, prolonged blood circulation time due to reduced clearance by the RES, and increased chances of reaching the disease site. Surface charge largely affects the interaction between NPs and cells. Compared to neutral and anionic NPs, cationic NPs displayed a high affinity for the cell membrane with a negative potential due to electrostatic interactions. Nonetheless, a high accumulation of cationic NPs causes perturbation of the cell membrane. The NPs transporting slightly negative charges were found to reduce their cytotoxic effect and interaction with plasma proteins, resulting in prolonged blood circulation. In addition, the elasticity of NPs (i.e., Young's modulus) is one of the critical properties in the optimization of the interaction between NPs and biological specimens. Soft NPs exhibit reduced interaction with immune cells and are not easily eliminated by RES. As a result, they displayed prolonged blood circulation as well as high extravasation into tumor tissues compared to hard NPs. Unequivocal conclusions from studies that investigated the effect of the physical properties of NPs on the pharmacokinetic features of NPs cannot be easily drawn. Notably, the physical properties and materials of NPs widely varied among the studies. This wide variation inherently imposes difficulty when performing a direct comparison among the results found across studies. Furthermore, the complexity of the pharmacokinetic behaviors of NPs and the heterogeneous nature of diseases, such as cancer, make it difficult

to evaluate the efficiency of NPs as drug delivery vehicles. However, rigorous scientific efforts are required to unveil the detailed impact of the physical properties of NPs on the pharmacokinetic features using in vitro and in vivo studies. Nevertheless, we can conclude that physical parameters, including size, shape, surface charge, and elasticity, should be optimized for the development of novel drug delivery systems using NPs with excellent biocompatibility and therapeutic efficacy.

Acknowledgements This research was supported by a National Research Foundation of Korea (NRF) grant funded by the Ministry of Education (NRF-2018R1D1A3B07050399).

Compliance with ethical standards

Conflicts of interest The authors declare that they have no conflicts of interest.

Research involving human and animal rights This article does not contain any studies involving human and animal subjects.

References

- Abdifetah O, Na-Bangchang K (2019) Pharmacokinetic studies of nanoparticles as a delivery system for conventional drugs and herb-derived compounds for cancer therapy: a systematic review. *Int J Nanomedicine* 14:5659–5677. <https://doi.org/10.2147/ijn.S213229>
- Agarwal R, Singh V, Jurney P, Shi L, Sreenivasan SV, Roy K (2013) Mammalian cells preferentially internalize hydrogel nanodiscs over nanorods and use shape-specific uptake mechanisms. *Proc Natl Acad Sci U S A* 110:17247–17252. <https://doi.org/10.1073/pnas.1305000110>
- Al-azzawi S, Masheta D (2019) Designing a drug delivery system for improved tumor treatment and targeting by functionalization of a cell-penetrating peptide. *J Pharm Investig* 49:643–654. <https://doi.org/10.1007/s40005-018-00424-w>
- Alberts B JA, Lewis J, et al. (2002) *Molecular Biology of the Cell* New York: Garland Science 4
- Alexander JF, Kozlovskaya V, Chen J, Kuncewicz T, Kharlampieva E, Godin B (2015) Cubical Shape Enhances the Interaction of Layer-by-Layer Polymeric Particles with Breast Cancer Cells. *Adv Healthc Mater* 4:2657–2666. <https://doi.org/10.1002/adhm.201500537>
- Anselmo AC, Zhang M, Kumar S, Vogus DR, Menegatti S, Helgeson ME, Mitragotri S (2015) Elasticity of nanoparticles influences their blood circulation, phagocytosis, endocytosis, and targeting. *ACS Nano* 9:3169–3177. <https://doi.org/10.1021/acsnano.5b00147>
- Arvizo RR et al (2010) Effect of nanoparticle surface charge at the plasma membrane and beyond. *Nano Lett* 10:2543–2548. <https://doi.org/10.1021/nl101140t>
- Bandyopadhyay S et al (2018) Growing gold nanostructures for shape-selective cellular uptake. *Nanoscale Res Lett* 13:254. <https://doi.org/10.1186/s11671-018-2662-7>
- Barenholz Y (2012) Doxil(R)—the first FDA-approved nano-drug lessons learned. *J Control Release* 160:117–134. <https://doi.org/10.1016/j.jconrel.2012.03.020>
- Bastatas L et al (2012) AFM nano-mechanics and calcium dynamics of prostate cancer cells with distinct metastatic potential. *Biochem Biophys Acta* 1820:1111–1120. <https://doi.org/10.1016/j.bbagen.2012.02.006>
- Behzadi S et al (2017) Cellular uptake of nanoparticles: journey inside the cell. *Chem Soc Rev* 46:4218–4244. <https://doi.org/10.1039/c6cs00636a>
- Bolean M et al (2017) Topographic analysis by atomic force microscopy of proteoliposomes matrix vesicle mimetics harboring TNAP and AnxA5. *Biochim Biophys Acta Biomembr* 1859:1911–1920. <https://doi.org/10.1016/j.bbamem.2017.05.010>
- Brochu H, Vermette P (2008) Young's moduli of surface-bound liposomes by atomic force microscopy force measurements. *Langmuir: the ACS journal of surfaces and colloids* 24:2009–2014. <https://doi.org/10.1021/la702382d>
- Cabral H et al (2011) Accumulation of sub-100 nm polymeric micelles in poorly permeable tumours depends on size. *Nat Nanotechnol* 6:815–823. <https://doi.org/10.1038/nnano.2011.166>
- Champion JA, Mitragotri S (2006) Role of target geometry in phagocytosis. *Proc Natl Acad Sci U S A* 103:4930–4934. <https://doi.org/10.1073/pnas.0600997103>
- Choi HS et al (2007) Renal clearance of quantum dots. *Nat Biotechnol* 25:1165–1170. <https://doi.org/10.1038/nbt1340>
- Crucho CIC, Barros MT (2017) Polymeric nanoparticles: A study on the preparation variables and characterization methods. *Mater Sci Eng C Mater Biol Appl* 80:771–784. <https://doi.org/10.1016/j.msec.2017.06.004>
- Cui J et al (2013) Mechanically tunable, self-adjuvanting nanoengineered polypeptide particles. *Adv Mater* 25:3468–3472. <https://doi.org/10.1002/adma.201300981>
- Cun X et al (2018) A size switchable nanoplatform for targeting the tumor microenvironment and deep tumor penetration. *Nanoscale* 10:9935–9948. <https://doi.org/10.1039/c8nr00640g>
- Davis ME, Chen ZG, Shin DM (2008) Nanoparticle therapeutics: an emerging treatment modality for cancer. *Nat Rev Drug Discov* 7:771–782. <https://doi.org/10.1038/nrd2614>
- Du XJ et al (2018) The effect of surface charge on oral absorption of polymeric nanoparticles. *Biomater Sci* 6:642–650. <https://doi.org/10.1039/c7bm01096f>
- Fang C, Shi B, Pei YY, Hong MH, Wu J, Chen HZ (2006) vivo tumor targeting of tumor necrosis factor-alpha-loaded stealth nanoparticles: effect of MePEG molecular weight and particle size. *Eur J Pharm Sci* 27:27–36. <https://doi.org/10.1016/j.ejps.2005.08.002>
- Geng Y, Dalhaimer P, Cai S, Tsai R, Tewari M, Minko T, Discher DE (2007) Shape effects of filaments versus spherical particles in flow and drug delivery. *Nat Nanotechnol* 2:249–255. <https://doi.org/10.1038/nnano.2007.70>
- Guo P et al (2018a) Nanoparticle elasticity directs tumor uptake *Nat Commun* 9:130. <https://doi.org/10.1038/s41467-017-02588-9>
- Guo Y et al (2018b) Shape of Nanoparticles as a Design Parameter to Improve Docetaxel Antitumor Efficacy. *Bioconj Chem* 29:1302–1311. <https://doi.org/10.1021/acs.bioconjchem.8b00059>
- Han S-M et al (2018) Improvement of cellular uptake of hydrophilic molecule, calcein, formulated by liposome. *J Pharm Investig* 48:595–601. <https://doi.org/10.1007/s40005-017-0358-0>
- Hartmann R, Weidenbach M, Neubauer M, Fery A, Parak WJ (2015) Stiffness-dependent in vitro uptake and lysosomal acidification of colloidal particles. *Angew Chem Int Ed Engl* 54:1365–1368. <https://doi.org/10.1002/anie.201409693>
- Hazarika A, Peretz E, Dikovskiy V, Santra PK, Shneck RZ, Sarma DD, Manassen Y (2014) STM verification of the reduction of the Young's modulus of CdS nanoparticles at smaller sizes. *Surf Sci* 630:89–95
- He C, Hu Y, Yin L, Tang C, Yin C (2010) Effects of particle size and surface charge on cellular uptake and biodistribution of

- polymeric nanoparticles. *Biomaterials* 31:3657–3666. <https://doi.org/10.1016/j.biomaterials.2010.01.065>
- Herant M, Heinrich V, Dembo M (2005) Mechanics of neutrophil phagocytosis: behavior of the cortical tension. *J Cell Sci* 118:1789–1797. <https://doi.org/10.1242/jcs.02275>
- Hillaireau H, Couvreur P (2009) Nanocarriers' entry into the cell: relevance to drug delivery. *Cell Mol Life Sci* 66:2873–2896. <https://doi.org/10.1007/s00018-009-0053-z>
- Huang X, Li L, Liu T, Hao N, Liu H, Chen D, Tang F (2011) The shape effect of mesoporous silica nanoparticles on biodistribution, clearance, and biocompatibility in vivo. *ACS Nano* 5:5390–5399. <https://doi.org/10.1021/nn200365a>
- Hung CC et al (2016) Active tumor permeation and uptake of surface charge-switchable theranostic nanoparticles for imaging-guided photothermal/chemo combinatorial therapy. *Theranostics* 6:302–317. <https://doi.org/10.7150/thno.13686>
- Ingham B et al (2010) Synchrotron x-ray diffraction measurements of strain in metallic nanoparticles with oxide shells. *J Phys D Appl Phys* 43:075301. <https://doi.org/10.1088/0022-3727/43/7/075301>
- Jain RK, Stylianopoulos T (2010) Delivering nanomedicine to solid tumors. *Nat Rev Clin Oncol* 7:653–664. <https://doi.org/10.1038/nrclinonc.2010.139>
- Javid J, Haeri A, Nowroozi F, Dadashzadeh S (2019) Pharmacokinetics, Tissue Distribution and Excretion of Ag2S Quantum Dots in Mice and Rats: the Effects of Injection Dose, Particle Size and Surface Charge. *Pharm Res* 36:46. <https://doi.org/10.1007/s11095-019-2571-1>
- Jeon S, Clavadetscher J, Lee DK, Chankeshwara SV, Bradley M, Cho WS (2018) Surface Charge-Dependent Cellular Uptake of Polystyrene Nanoparticles. *Nanomaterials (Basel, Switzerland)* 8(12):1028. <https://doi.org/10.3390/nano8121028>
- Kang JH, Jang WY, Ko YT (2017) The Effect of Surface Charges on the Cellular Uptake of Liposomes Investigated by Live Cell Imaging. *Pharm Res* 34:704–717. <https://doi.org/10.1007/s11095-017-2097-3>
- Ke W et al (2019) Length effect of stimuli-responsive block copolymer prodrug filomicelles on drug delivery efficiency. *J Control Release* 318:67–77. <https://doi.org/10.1016/j.jconrel.2019.12.012>
- Key J et al (2015) Soft Discoidal Polymeric Nanoconstructs Resist Macrophage Uptake and Enhance Vascular Targeting in Tumors. *ACS Nano* 9:11628–11641. <https://doi.org/10.1021/acs.nano.5b04866>
- Kim D-H, Lee S-E, Pyo Y-C, Tran P, Park J-S (2020) Solubility enhancement and application of cyclodextrins in local drug delivery. *J Pharm Investig* 50:17–27. <https://doi.org/10.1007/s40005-019-00434-2>
- Kobayashi H, Watanabe R, Choyke PL (2013) Improving conventional enhanced permeability and retention (EPR) effects; what is the appropriate target? *Theranostics* 4:81–89. <https://doi.org/10.7150/thno.7193>
- Koga J, Matoba T, Egashira K (2016) Anti-inflammatory Nanoparticle for Prevention of Atherosclerotic Vascular Diseases. *J Atheroscler Thromb* 23:757–765. <https://doi.org/10.5551/jat.35113>
- Kolhar P, Anselmo AC, Gupta V, Pant K, Prabhakarpanian B, Ruoslahti E, Mitragotri S (2013) Using shape effects to target antibody-coated nanoparticles to lung and brain endothelium. *Proc Natl Acad Sci U S A* 110:10753–10758. <https://doi.org/10.1073/pnas.1308345110>
- Le Q-V, Choi J, Oh Y-K (2018) Nano delivery systems and cancer immunotherapy. *J Pharm Investig* 48:527–539. <https://doi.org/10.1007/s40005-018-0399-z>
- Lee M-K (2019) Clinical usefulness of liposomal formulations in cancer therapy: lessons from the experiences of doxorubicin. *J Pharm Investig* 49:203–214. <https://doi.org/10.1007/s40005-018-0398-0>
- Lesniak A, Salvati A, Santos-Martinez MJ, Radomski MW, Dawson KA, Åberg C (2013) Nanoparticle adhesion to the cell membrane and its effect on nanoparticle uptake efficiency. *J Am Chem Soc* 135:1438–1444. <https://doi.org/10.1021/ja309812z>
- Li L, Liu T, Fu C, Tan L, Meng X, Liu H (2015) Biodistribution, excretion, and toxicity of mesoporous silica nanoparticles after oral administration depend on their shape. *Nanomedicine* 11:1915–1924. <https://doi.org/10.1016/j.nano.2015.07.004>
- Li L et al (2019) Unexpected Size Effect: The Interplay between Different-Sized Nanoparticles in Their Cellular Uptake. *Small* 15:e1901687. <https://doi.org/10.1002/smll.201901687>
- Liang X, Mao G, Ng KY (2004) Mechanical properties and stability measurement of cholesterol-containing liposome on mica by atomic force microscopy. *J Colloid Interface Sci* 278:53–62. <https://doi.org/10.1016/j.jcis.2004.05.042>
- Liu Q, Li H, Xia Q, Liu Y, Xiao K (2015) Role of surface charge in determining the biological effects of CdSe/ZnS quantum dots. *Int J Nanomedicine* 10:7073–7088. <https://doi.org/10.2147/ijn.S94543>
- Liu W, Zhou X, Mao Z, Yu D, Wang B, Gao C (2012) Uptake of hydrogel particles with different stiffness and its influence on HepG2 cell functions. *Soft Matter* 8:9235–9245. <https://doi.org/10.1039/C2SM26001H>
- Liu Y, Hardie J, Zhang X, Rotello VM (2017) Effects of engineered nanoparticles on the innate immune system. *Semin Immunol* 34:25–32. <https://doi.org/10.1016/j.smim.2017.09.011>
- Liu Y, Ji M, Wong MK, Joo KI, Wang P (2013) Enhanced therapeutic efficacy of iRGD-conjugated crosslinked multilayer liposomes for drug delivery. *Biomed Res Int* 2013:378380. <https://doi.org/10.1155/2013/378380>
- Lu F, Wu SH, Hung Y, Mou CY (2009) Size effect on cell uptake in well-suspended, uniform mesoporous silica nanoparticles. *Small* 5:1408–1413. <https://doi.org/10.1002/smll.200900005>
- Mahaffy RE, Park S, Gerde E, Kas J, Shih CK (2004) Quantitative analysis of the viscoelastic properties of thin regions of fibroblasts using atomic force microscopy. *Biophys J* 86:1777–1793. [https://doi.org/10.1016/s0006-3495\(04\)74245-9](https://doi.org/10.1016/s0006-3495(04)74245-9)
- Mangan C, Stott MC, Dhanda R (2018) Renal physiology: blood flow, glomerular filtration and plasma clearance. *Anaesth Intensive Care medicine* 19:254–257. <https://doi.org/10.1016/j.mpaic.2018.02.013>
- Masserini M (2013) Nanoparticles for brain drug delivery. *ISRN Biochem* 2013:238428. <https://doi.org/10.1155/2013/238428>
- Meng R, Li K, Chen Z, Shi C (2016) Multilayer Coating of Tetrandrine-loaded PLGA nanoparticles: Effect of surface charges on cellular uptake rate and drug release profile. *J Huazhong Univ Sci Technolog Med Sci* 36:14–20. <https://doi.org/10.1007/s11596-016-1535-5>
- Merkel TJ et al (2011) Using mechanobiological mimicry of red blood cells to extend circulation times of hydrogel microparticles. *Proc Natl Acad Sci U S A* 108:586–591. <https://doi.org/10.1073/pnas.1010013108>
- Miao L, Huang L (2015) Exploring the tumor microenvironment with nanoparticles. *Cancer Treat Res* 166:193–226. https://doi.org/10.1007/978-3-319-16555-4_9
- Mullner M, Dodds SJ, Nguyen TH, Senyschyn D, Porter CJ, Boyd BJ, Caruso F (2015) Size and rigidity of cylindrical polymer brushes dictate long circulating properties in vivo. *ACS Nano* 9:1294–1304. <https://doi.org/10.1021/mn505125f>
- Nagayama S, Ogawara K, Fukuoka Y, Higaki K, Kimura T (2007) Time-dependent changes in opsonin amount associated on nanoparticles alter their hepatic uptake characteristics. *Int J Pharm* 342:215–221. <https://doi.org/10.1016/j.ijpharm.2007.04.036>
- Naguib YW, Rodriguez BL, Li X, Hursting SD, Williams RO 3rd, Cui Z (2014) Solid lipid nanoparticle formulations of docetaxel prepared with high melting point triglycerides: in vitro and in vivo

- evaluation. *Mol Pharm* 11:1239–1249. <https://doi.org/10.1021/mp4006968>
- Ohlson M, Sörensson J, Haraldsson B (2001) A gel-membrane model of glomerular charge and size selectivity in series. *Am J Physiol Renal Physiol* 280:F396–405. <https://doi.org/10.1152/ajprenal.2001.280.3.F396>
- Pada AK, Desai D, Sun K, Prakirth Govardhanam N, Tornquist K, Zhang J, Rosenholm JM (2019) Comparison of Polydopamine-Coated Mesoporous Silica Nanorods and Spheres for the Delivery of Hydrophilic and Hydrophobic Anticancer Drugs. *Int J Mol Sci*. <https://doi.org/10.3390/ijms20143408>
- Patel T, Zhou J, Piepmeier JM, Saltzman WM (2012) Polymeric nanoparticles for drug delivery to the central nervous system. *Adv Drug Deliv Rev* 64:701–705. <https://doi.org/10.1016/j.addr.2011.12.006>
- Perry JL, Reuter KG, Luft JC, Pecot CV, Zamboni W, DeSimone JM (2017) Mediating Passive Tumor Accumulation through Particle Size, Tumor Type, and Location. *Nano Lett* 17:2879–2886. <https://doi.org/10.1021/acs.nanolett.7b00021>
- Pi HJ, Park S, Lee J, Lee KJ (2000) Superlattice, rhombus, square, and hexagonal standing waves in magnetically driven ferrofluid surface. *Phys Rev Lett* 84:5316–5319. <https://doi.org/10.1103/PhysRevLett.84.5316>
- Probst CE, Zrazhevskiy P, Bagalkot V, Gao X (2013) Quantum dots as a platform for nanoparticle drug delivery vehicle design. *Adv Drug Deliv Rev* 65:703–718. <https://doi.org/10.1016/j.addr.2012.09.036>
- Qian X et al (2019) Targeting and microenvironment-improving of phenylboronic acid-decorated soy protein nanoparticles with different sizes to tumor. *Theranostics* 9:7417–7430. <https://doi.org/10.7150/thno.33470>
- Rejman J, Oberle V, Zuhorn IS, Hoekstra D (2004) Size-dependent internalization of particles via the pathways of clathrin- and caveolae-mediated endocytosis. *Biochem J* 377:159–169. <https://doi.org/10.1042/bj20031253>
- Saw WS et al (2018) Size-dependent effect of cystine/citric acid-capped confetto-like gold nanoparticles on cellular uptake and photothermal cancer therapy. *Colloids Surf B Biointerfaces* 161:365–374. <https://doi.org/10.1016/j.colsurfb.2017.10.064>
- Shao D et al (2017) The shape effect of magnetic mesoporous silica nanoparticles on endocytosis, biocompatibility and biodistribution. *Acta Biomater* 49:531–540. <https://doi.org/10.1016/j.actbio.2016.11.007>
- Shao XR et al (2015) Independent effect of polymeric nanoparticle zeta potential/surface charge, on their cytotoxicity and affinity to cells. *Cell Prolif* 48:465–474. <https://doi.org/10.1111/cpr.12192>
- Shen J-M, Yin T, Tian X-Z, Gao F-Y, Xu S (2013) Surface Charge-Switchable Polymeric Magnetic Nanoparticles for the Controlled Release of Anticancer Drug. *ACS Appl Mater Interfaces* 5:7014–7024. <https://doi.org/10.1021/am401277s>
- Shen J, Zhao L, Han G (2013) Lanthanide-doped upconverting luminescent nanoparticle platforms for optical imaging-guided drug delivery and therapy. *Adv Drug Deliv Rev* 65:744–755. <https://doi.org/10.1016/j.addr.2012.05.007>
- Shukla S et al (2015) The Impact of Aspect Ratio on the Biodistribution and Tumor Homing of Rigid Soft-Matter Nanorods. *Adv Healthc Mater* 4:874–882. <https://doi.org/10.1002/adhm.201400641>
- Singh D, Bedi N, Tiwary AK (2018) Enhancing solubility of poorly aqueous soluble drugs: critical appraisal of techniques. *J Pharm Investig* 48:509–526. <https://doi.org/10.1007/s40005-017-0357-1>
- Sobh RA, Nasr HE, Moustafa AB, Mohamed WS (2019) Tailoring of anticancer drugs loaded in MWCNT/Poly(MMA-co-HEMA) nanosphere composite by using in situ microemulsion polymerization. *J Pharm Investig* 49:45–55. <https://doi.org/10.1007/s40005-018-0390-8>
- Sonavane G, Tomoda K, Makino K (2008) Biodistribution of colloidal gold nanoparticles after intravenous administration: effect of particle size. *Colloids and surfaces B. Biointerfaces* 66:274–280. <https://doi.org/10.1016/j.colsurfb.2008.07.004>
- Song Y, Chen L (2015) Effect of net surface charge on physical properties of the cellulose nanoparticles and their efficacy for oral protein delivery. *Carbohydr Polym* 121:10–17. <https://doi.org/10.1016/j.carbpol.2014.12.019>
- Sousa F, Castro P, Fonte P, Kennedy PJ, Neves-Petersen MT, Sarmiento B (2017) Nanoparticles for the delivery of therapeutic antibodies: Dogma or promising strategy? *Expert Opin Drug Deliv* 14:1163–1176. <https://doi.org/10.1080/17425247.2017.1273345>
- Su YL, Fang JH, Liao CY, Lin CT, Li YT, Hu SH (2015) Targeted Mesoporous Iron Oxide Nanoparticles-Encapsulated Perfluorohexane and a Hydrophobic Drug for Deep Tumor Penetration and Therapy. *Theranostics* 5:1233–1248. <https://doi.org/10.7150/thno.12843>
- Sun H et al (2015a) The role of capsule stiffness on cellular processing. *Chem Sci* 6:3505–3514. <https://doi.org/10.1039/c5sc00416k>
- Sun J et al (2015b) Tunable rigidity of (polymeric core)-(lipid shell) nanoparticles for regulated cellular uptake. *Adv Mater* 27:1402–1407. <https://doi.org/10.1002/adma.201404788>
- Sun XY, Gan QZ, Ouyang JM (2017) Size-dependent cellular uptake mechanism and cytotoxicity toward calcium oxalate on Vero cells. *Sci Rep* 7:41949. <https://doi.org/10.1038/srep41949>
- Taghipour-Sabzevar V, Sharifi T, Moghaddam MM (2019) Polymeric nanoparticles as carrier for targeted and controlled delivery of anticancer agents. *Ther Deliv* 10:527–550. <https://doi.org/10.4155/tde-2019-0044>
- Takechi-Haraya Y, Goda Y, Izutsu K, Sakai-Kato K (2019) Improved Atomic Force Microscopy Stiffness Measurements of Nanoscale Liposomes by Cantilever Tip Shape Evaluation. *Anal Chem* 91:10432–10440. <https://doi.org/10.1021/acs.analchem.9b00250>
- Takechi-Haraya Y, Goda Y, Sakai-Kato K (2018) Atomic Force Microscopy Study on the Stiffness of Nanosized Liposomes Containing Charged Lipids. *Langmuir: the ACS journal of surfaces and colloids* 34:7805–7812. <https://doi.org/10.1021/acs.langmuir.8b01121>
- Talamini L et al (2017) Influence of Size and Shape on the Anatomical Distribution of Endotoxin-Free Gold Nanoparticles. *ACS Nano* 11:5519–5529. <https://doi.org/10.1021/acsnano.7b00497>
- Tang Y, Han S, Liu H, Chen X, Huang L, Li X, Zhang J (2013) The role of surface chemistry in determining in vivo biodistribution and toxicity of CdSe/ZnS core-shell quantum dots. *Biomaterials* 34:8741–8755. <https://doi.org/10.1016/j.biomaterials.2013.07.087>
- Tavares AJ et al (2017) Effect of removing Kupffer cells on nanoparticle tumor delivery. *Proc Natl Acad Sci U S A* 114:E10871–e10880. <https://doi.org/10.1073/pnas.1713390114>
- Tchoryk A et al (2019) Penetration and Uptake of Nanoparticles in 3D Tumor Spheroids. *Bioconjug Chem* 30:1371–1384. <https://doi.org/10.1021/acs.bioconjchem.9b00136>
- Teschke O, de Souza EF (2002) Liposome Structure Imaging by Atomic Force Microscopy: Verification of Improved Liposome Stability during Adsorption of Multiple Aggregated Vesicles. *Langmuir: the ACS journal of surfaces and colloids* 18:6513–6520. <https://doi.org/10.1021/la025689v>
- Uribe-Querol E, Rosales C (2017) Control of Phagocytosis by Microbial Pathogens. *Front Immunol* 8:1368. <https://doi.org/10.3389/fimmu.2017.01368>
- Utreja P, Jain S, Tiwary AK (2011) Localized delivery of paclitaxel using elastic liposomes: formulation development and evaluation. *Drug Deliv* 18:367–376. <https://doi.org/10.3109/10717544.2011.558527>
- Van den Hoven JM, Van Tomme SR, Metselaar JM, Nuijen B, Beijnen JH, Storm G (2011) Liposomal drug formulations in the

- treatment of rheumatoid arthritis. *Mol Pharm* 8:1002–1015. <https://doi.org/10.1021/mp2000742>
- Van Furth R, Cohn ZA, Hirsch JG, Humphrey JH, Spector WG, Langevoort HL (1972) The mononuclear phagocyte system: a new classification of macrophages, monocytes, and their precursor cells. *Bull World Health Organ* 46:845–852
- Ventola CL (2017) Progress in Nanomedicine: Approved and Investigational. *Nanodrugs* 42:742–755
- Verma AK, Kumar A (2013) Pharmacokinetics and biodistribution of negatively charged pectin nanoparticles encapsulating paclitaxel. *Cancer Nanotechnol* 4:99–102. <https://doi.org/10.1007/s12645-013-0041-8>
- Vio V, Marchant MJ, Araya E, Kogan MJ (2017) Metal Nanoparticles for the Treatment and Diagnosis of Neurodegenerative Brain Diseases. *Curr Pharm Des* 23:1916–1926. <https://doi.org/10.2174/1381612823666170105152948>
- Wang EC, Wang AZ (2014) Nanoparticles and their applications in cell and molecular biology. *Integr Biol (Camb)* 6:9–26. <https://doi.org/10.1039/c3ib40165k>
- Wang JY et al (2016) Effects of surface charges of gold nanoclusters on long-term in vivo biodistribution, toxicity, and cancer radiation therapy. *Int J Nanomedicine* 11:3475–3485. <https://doi.org/10.2147/ijn.S106073>
- Wang P, Wang X, Wang L, Hou X, Liu W, Chen C (2015) Interaction of gold nanoparticles with proteins and cells *Sci Technol. Adv Mater* 16:034610. <https://doi.org/10.1088/1468-6996/16/3/034610>
- Xiang S, Tong H, Shi Q, Fernandes JC, Jin T, Dai K, Zhang X (2012) Uptake mechanisms of non-viral gene delivery. *J Control Release* 158:371–378. <https://doi.org/10.1016/j.jconrel.2011.09.093>
- Xiao K et al (2011) The effect of surface charge on in vivo biodistribution of PEG-oligocholic acid based micellar nanoparticles. *Biomaterials* 32:3435–3446. <https://doi.org/10.1016/j.biomaterials.2011.01.021>
- Yang M, Brackenbury WJ (2013) Membrane potential and cancer progression. *Front Physiol* 4:185–185. <https://doi.org/10.3389/fphys.2013.00185>
- Yu Z, Fan W, Wang L, Qi J, Lu Y, Wu W (2019) Effect of Surface Charges on Oral Absorption of Intact Solid Lipid Nanoparticles. *Mol Pharm.* <https://doi.org/10.1021/acs.molpharmaceut.9b00861>
- Zhang D, Wei L, Zhong M, Xiao L, Li HW, Wang J (2018) The morphology and surface charge-dependent cellular uptake efficiency of upconversion nanostructures revealed by single-particle optical microscopy. *Chem Sci* 9:5260–5269. <https://doi.org/10.1039/c8sc01828f>
- Zhang H, Liu Y, Chen M, Luo X, Li X (2016) Shape effects of electrospun fiber rods on the tissue distribution and antitumor efficacy. *J Control Release* 244:52–62. <https://doi.org/10.1016/j.jconrel.2016.05.011>
- Zhang L et al (2015) Microfluidic Synthesis of Hybrid Nanoparticles with Controlled Lipid Layers: Understanding Flexibility-Regulated Cell-Nanoparticle Interaction. *ACS Nano* 9:9912–9921. <https://doi.org/10.1021/acs.nano.5b05792>
- Zhang Y et al (2008) Zeta potential: a surface electrical characteristic to probe the interaction of nanoparticles with normal and cancer human breast epithelial cells. *Biomed Microdevices* 10:321–328. <https://doi.org/10.1007/s10544-007-9139-2>
- Zhang Z, Liu C, Li C, Wu W, Jiang X (2019) Shape Effects of Cylindrical versus Spherical Unimolecular Polymer Nanomaterials on in Vitro and in Vivo. *Behaviors Research (Wash D C)* 2019:2391486. <https://doi.org/10.34133/2019/2391486>
- Zhao J, Chai YD, Zhang J, Huang PF, Nakashima K, Gong YK (2015) Long circulating micelles of an amphiphilic random copolymer bearing cell outer membrane phosphorylcholine zwitterions. *Acta Biomater* 16:94–102. <https://doi.org/10.1016/j.actbio.2015.01.019>
- Zheng N, Li J, Xu C, Xu L, Li S, Xu L (2018) Mesoporous silica nanorods for improved oral drug absorption *Artif Cells Nanomed. Biotechnol* 46:1132–1140. <https://doi.org/10.1080/21691401.2017.1362414>

Publisher's Note Springer Nature remains neutral with regard to jurisdictional claims in published maps and institutional affiliations.